

RESEARCH ARTICLE

Protective ventilation in a pig model of acute lung injury: timing is as important as pressure

Harry Ramcharran,¹  Jason H. T. Bates,⁴  Joshua Satalin,¹ Sarah Blair,¹ Penny L. Andrews,² Donald P. Gaver,³ Louis A. Gatto,¹ Guirong Wang,¹ Auyon J. Ghosh,¹ Benjamin Robedee,¹ James Vossler,¹ Nader M. Habashi,² Nirav Daphtry,⁴ Michaela Kollisch-Singule,¹ and  Gary F. Nieman¹

¹SUNY Upstate Medical University, Syracuse, New York; ²R Adams Cowley Shock Trauma Center, Baltimore, Maryland;

³Tulane University, New Orleans, Louisiana; and ⁴University of Vermont, Burlington, Vermont

Abstract

Ventilator-induced lung injury (VILI) is a significant risk for patients with acute respiratory distress syndrome (ARDS). Management of the patient with ARDS is currently dominated by the use of low tidal volume mechanical ventilation, the presumption being that this mitigates overdistension (OD) injury to the remaining normal lung tissue. Evidence exists, however, that it may be more important to avoid cyclic recruitment and derecruitment (RD) of lung units, although the relative roles of OD and RD in VILI remain unclear. Forty pigs had a heterogeneous lung injury induced by Tween instillation and were randomized into four groups ($n = 10$ each) with higher (\uparrow) or lower (\downarrow) levels of OD and/or RD imposed using airway pressure release ventilation (APRV). OD was increased by setting inspiratory airway pressure to 40 cmH₂O and lessened with 28 cmH₂O. RD was attenuated using a short duration of expiration (~ 0.45 s) and increased with a longer duration (~ 1.0 s). All groups developed mild ARDS following injury. RD \uparrow OD \uparrow caused the greatest degree of lung injury as determined by $\text{PaO}_2/\text{FiO}_2$ ratio (226.1 ± 41.4 mmHg). RD \uparrow OD \downarrow ($\text{PaO}_2/\text{FiO}_2 = 333.9 \pm 33.1$ mmHg) and RD \downarrow OD \uparrow ($\text{PaO}_2/\text{FiO}_2 = 377.4 \pm 43.2$ mmHg) were both moderately injurious, whereas RD \downarrow OD \downarrow ($\text{PaO}_2/\text{FiO}_2 = 472.3 \pm 22.2$ mmHg; $P < 0.05$) was least injurious. Both tidal volume and driving pressure were essentially identical in the RD \uparrow OD \downarrow and RD \downarrow OD \uparrow groups. We, therefore, conclude that considerations of expiratory time may be at least as important as pressure for safely ventilating the injured lung.

NEW & NOTEWORTHY In a large animal model of ARDS, recruitment/derecruitment caused greater VILI than overdistension, whereas both mechanisms together caused severe lung damage. These findings suggest that eliminating cyclic recruitment and derecruitment during mechanical ventilation should be a preeminent management goal for the patient with ARDS. The airway pressure release ventilation (APRV) mode of mechanical ventilation can achieve this if delivered with an expiratory duration (T_{Low}) that is brief enough to prevent derecruitment at end expiration.

acute respiratory distress syndrome (ARDS); heterogeneous lung injury; overdistension; recruitment/derecruitment; ventilator-induced lung injury (VILI)

INTRODUCTION

The acute respiratory distress syndrome (ARDS) is a common and frequently fatal condition that is managed medically (1). Mechanical ventilation is a cornerstone of this management, but if applied incorrectly, can cause ventilator-induced lung injury (VILI). Although low tidal volume ventilation is generally thought to be protective against VILI and remains the standard of care for ARDS, mortality remains unacceptably high (2). Although the reasons for these poor outcomes are unclear, evidence is accumulating that overdistension (OD) of normal lung tissue due to high airway pressures causes minimal lung injury on its own (3, 4). Instead, cyclic intratidal recruitment and derecruitment (RD) of lung units may actually be the instigating factor in VILI (5) because of the damaging stresses that are

applied to derecruited lung tissue each time apposed epithelial surfaces are peeled apart during inspiration (6–9). This implies that avoidance of RD during mechanical ventilation is a preeminent management goal for the patient with ARDS.

The traditional approach to avoiding RD is to apply positive end-expiratory pressure (PEEP), the idea being that this will open the lung and keep the expiratory lung volume above the level where derecruitment occurs (10). Unfortunately, there may be no safe level of positive end-expiratory pressure (PEEP) for which this applies, particularly in a severely injured lung (11), as evidenced by decremental PEEP studies in patients with acute lung injury (12). The disassociation between PEEP and RD exists because RD is not determined simply by the pressure applied to the lungs; it is also a function of time. That is, lung units take a finite, and sometimes a very short, amount of time to close when pressure is reduced

Correspondence: J. Satalin (satalinj@upstate.edu).

Submitted 1 June 2022 / Revised 26 August 2022 / Accepted 19 September 2022

because closure involves the local flow of airway lining fluid to form airway plugs or to fill alveoli. Similarly, units take time to reopen when pressure is raised because of the local flows needed to displace the occluding fluid (13–17).

The above considerations imply that controlling RD during mechanical ventilation is not simply a matter of controlling pressure. The temporal aspects of the ventilatory waveform also have a major bearing on how much RD takes place over a breath. Dissecting the relative roles of pressure and timing, however, requires that they be controlled independently of each other, which is a significant challenge with most modes of mechanical ventilation. Airway pressure release ventilation (APRV), on the other hand, does permit some degree of separation between pressure and timing because of the simplicity of its structure; inspiration and expiration are each produced by a fixed pressure applied for a set period of time, and these four quantities (two pressures and two durations) can be varied independently of each other. Furthermore, computational modeling suggests that exploiting this feature of APRV to account for the time dependence of derecruitment has the potential to significantly mitigate VILI (18). The purpose of the present study was therefore to use APRV in a translational pig model of ARDS to separate the contributions of pressure, volume, and timing to the generation of VILI during the early phase of ARDS.

METHODS

All experiments were conducted with approval from the State University of New York Upstate Medical University Institutional Animal Care and Use Committee in accordance with ARRIVE guidelines.

Surgical Preparation and Baseline Measurements

Female Yorkshire pigs (38.3 ± 1.8 kg) ~6 mo of age were anesthetized with intravenous ketamine (90 mg/kg) and xylazine (10 mg/kg). A tracheostomy was performed with a 7.5-mm endotracheal tube (Harvard Apparatus) and connected to a mechanical ventilator (Dräger Evita Infinity V500) with baseline settings of a tidal volume (V_T) of 10 mL/kg, respiratory rate (RR) of 12 breaths/min, positive end-expiratory pressure (PEEP) of 5 cmH₂O, and a fraction of inspired oxygen (F_{iO_2}) of 100%. Central venous catheters were placed in both external jugular veins for the administration of fluids and medications. A VolumeView catheter (Edwards Lifesciences, Irvine) was placed in the femoral artery and used for arterial blood pressure monitoring and blood gas (ABG) measurements (cobas b 221, Roche). The VolumeView catheter was attached to an EV110 acquisition device (Edwards Lifesciences, Irvine) to calculate cardiac parameters, pulmonary edema and pulmonary vascular permeability index via the thermodilution method.

Study Protocol

The animals were transitioned to continuous positive airway pressure (CPAP) equivalent to their baseline plateau pressure of 20 cmH₂O. The airway was visualized with a bronchoscope, which was advanced down the right mainstem bronchus past the right middle lobe bronchus (19). This allowed precise instillation of a 3% Tween-20 detergent

solution (0.75 mL/kg) into only the dependent basilar lung regions to deactivate pulmonary surfactant and thus simulate ARDS pathophysiology (20). The bronchoscope was then withdrawn to the carina and then advanced down the left mainstem bronchus just past the left cranial lobe bronchus (19) so that another (0.75 mL/kg) Tween dose could be administered locally. The animals were paralyzed with rocuronium and ventilated with the airway pressure release ventilation (APRV) mode.

We studied four groups of animals with $n = 10$ animals per group. This number was chosen using the Pa_{O_2}/F_{iO_2} ratio as the primary outcome. In a previous study of a similar animal model (21), we found that a group of control animals had a mean Pa_{O_2}/F_{iO_2} of 144 mmHg with a standard deviation of 142 mmHg. A standard power calculation revealed that we would need 10 animal per group to show a significant difference between this value of Pa_{O_2}/F_{iO_2} and the ARDS-definitive value of 300 mmHg with a Type I error of 5% and a power of 80%. The ventilator settings in the various groups of the present study were designed to either increase (↑) or decrease (↓) RD and OD. These groups are designated as: 1) OD↓ RD↓, 2) OD↓ RD↑, 3) OD↑ RD↓, and 4) OD↑ RD↑. The investigators involved in conducting the experiments were not blinded to treatment groups.

APRV is a pressure-controlled mode of mechanical ventilation defined by four parameters: 1) the value of the constant pressure applied to the airway opening during inspiration (P_{High}), 2) the duration of inspiration (T_{High}), 3) the constant pressure applied during expiration (P_{Low}), and 4) the duration of expiration (T_{Low}). These parameters were chosen as follows:

- OD↑ was generated by setting $P_{High} = 40$ cmH₂O, since this has been shown to cause overdistention of lung tissue (22),
- OD↓ was induced with $P_{High} = 28$ cmH₂O, which is less than the plateau pressure limit of 30 cmH₂O recommended by clinical guidelines (10),
- RD↑ was generated by extending T_{Low} so that lung units had time to collapse prior to the start of the subsequent inspiration, and
- RD↓ was instigated by using a short T_{Low} designed to prevent the lungs from having enough time to derecruit during expiration.

The method used to determine the value of T_{Low} that controls RD has been described in detail previously (23). Briefly, expiration is terminated when the magnitude of expiratory flow has dropped to a specified percentage of its peak value, the latter being achieved at the beginning of expiration. We used a terminal expiratory flow of 75% of peak to produce a short T_{Low} that leads to RD↓, and terminal flow of 25% of peak to produce a long T_{Low} that leads to RD↑ (21). Figure 1 shows examples of the tracheal pressure and flow waveforms generated by the above realizations of APRV.

Baseline measurements of physiological parameters (see Table 1) were made at the start of the experimental protocol and then at the time point designated $T0$ immediately after Tween instillation. Additional sets of measurements were made every hour subsequently for the next 6 h (time points $T1$ through $T6$). Animals were provided 2 L of Lactated Ringer's solution before lung injury as a prophylactic against induced systemic hypotension. Additional boluses were

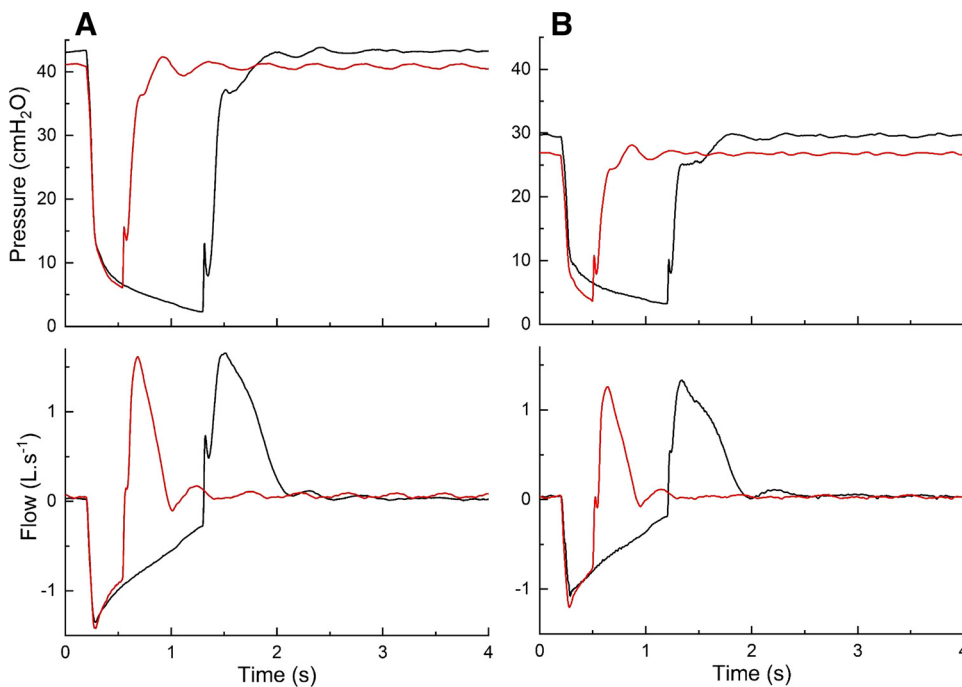


Figure 1. Examples of airway pressure and flow signals during APRV in a pig. A: black traces correspond to $OD \uparrow RD \uparrow$ and red traces correspond to $OD \uparrow RD \downarrow$. B: black traces correspond to $OD \downarrow RD \uparrow$ and $OD \downarrow RD \downarrow$. APRV, airway pressure release ventilation; OD, overdistension; RD, recruitment/derecruitment.

administered to maintain mean arterial pressure (MAP) > 65 mmHg after demonstration of fluid responsiveness. Lack of fluid responsiveness was identified by the requirement for two boluses within 1 h to maintain MAP > 65 mmHg, in which case a norepinephrine infusion was started. Inspired oxygen fraction (Fl_{O_2}) was titrated to a minimum of 30% if oxygenation improved, with goal oxygen saturation $> 90\%$.

Physiologic Parameter Measurement

Oscillometric measurements of respiratory system mechanics were made using a custom designed and built device consisting of a loudspeaker (Boss Audio CXX12 Subwoofer-100 Watts, Oxnard, CA) encased in a PVC and plexiglass chamber. The front of the chamber was connected laterally to the ventilator circuit with a plastic tube. A similar length of tubing connected the front and back of the chamber so that slowly varying circuit pressures due to mechanical ventilation could equilibrate either side of the speaker cone to prevent it from being driven to the end of its travel during inspiration. The speaker was driven with a superposition of 7 sinewaves having mutually prime frequencies of 5, 7, 11, 13, 17, and 19 Hz and amplitudes that maintained peak-to-peak flow roughly constant over this frequency range. The speaker was controlled by a power amplifier (Pyle PRO PTA 1000, Brooklyn, NY) and the data were low-pass filtered at 30 Hz and sampled at 100 Hz using a 16-bit A/D converter (NI USB-6212 (BNC) DAQ, National Instruments, Austin, TX). The driving of the speaker and the acquisition of data were implemented using Labview (National Instruments, TX).

Ten epochs of forced oscillatory flow were applied to the ventilator circuit every hour just before a pneumotachograph (Hans Rudolph, 3700 Series 0–160 L/min) that measured airway flow and a piezoresistive pressure sensor system (SC-24, Scireq, Montreal) that measured airway pressure. The oscillatory flow and pressure signals were high-pass filtered from the total signals to isolate them from the

ventilator waveforms and then respiratory system impedance was calculated as the ratio of the averaged cross and auto power spectra of pressure and flow in the frequency domain using a 1 s window length with 50% overlapping. The single-compartment resistance-elastance-inertance model of the respiratory system having impedance, $Z(f)$, given by

$$Z(f) = R_{rs} + i \left(2\pi f I_{rs} - \frac{E_{rs}}{2\pi f} \right) \quad (1)$$

was fit to the impedance spectra from 5 to 19 Hz, where R_{rs} is respiratory system resistance, I_{rs} is respiratory system inertance, E_{rs} is respiratory system elastance, and $i = +\sqrt{-1}$. This single-compartment model neglects the inter-cycle hysteresis from viscoelastic effects related to respiratory system tissue, surfactant transport, and regional mechanical heterogeneities throughout the lung (24). Nevertheless, the single-compartment model described by Eq. 1 captured the general shape of $Z(f)$ from 5 to 19 Hz (see example in Fig. 2). E_{rs} obtained in this way thus provided a robust estimate of overall respiratory system elastance, which is a good reflection of the mechanical status of the lung.

The inverse of E_{rs} , respiratory system compliance (C_{rs}), was taken as the outcome measure reflective of respiratory system mechanics and was normalized to its value at T_0 (nC_{rs}). This normalization is important because each ventilation group operates around different mean pressures, which means that direct comparison of C_{rs} between groups is not meaningful. However, the temporal response of nC_{rs} provides insight into pulmonary mechanical recovery of each group in a manner that can be compared. The investigator performing the analysis of oscillometry data (JHTB) was blinded to the treatment groups.

Oxygen saturation, MAP, heart rate, and temperature were continuously monitored (IntelliVue MP90, Philips Healthcare, Irvine, CA) and recorded hourly. Arterial blood gases were measured hourly (pH, Pa_{O_2} , PCO_2 , oxygen

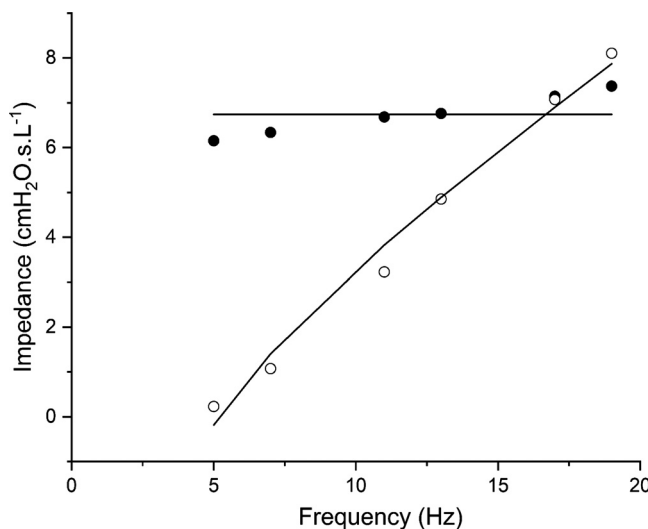


Figure 2. Example fit of Eq. 1 to $Z(f)$ data. Closed symbols—real part of impedance; open symbols—imaginary part of impedance; and solid lines—model fit.

saturation, electrolytes, and $\text{Pa}_{\text{O}_2}/\text{Fl}_{\text{O}_2}$ ratio). Ventilatory (peak inspiratory/plateau pressure, mean airway pressure, tidal volume, resistance, P_{High} , P_{Low} , T_{High} , T_{Low}) and VolumeView parameters (cardiac output, extravascular lung water, pulmonary vascular permeability index, global end-diastolic volume) were acquired hourly. Positive end-expiratory pressure (PEEP) was measured following a 6 s expiratory hold maneuver. Driving pressure (ΔP) was calculated as the difference between plateau and positive end-expiratory pressure.

Postmortem Studies

After 6 h of ventilation, the protocol was terminated, the animals euthanized (pentobarbital solution), and necropsy was performed. Bronchoalveolar lavage fluid (BALF) and lung tissue were collected and frozen, lung tissue was fixed in formalin for histopathology, and edema was assessed by a lung tissue wet/dry weight ratio (W/D). The lungs were excised and inflated to 25 cmH_2O , using stepwise increases in CPAP, for lung volume history standardization. Gross photos were taken at 25 cmH_2O inflation pressure and a photo of the cut surface of the basilar lobe was taken. A tissue section from the left apical lobe (non-Tween-injured tissue) and the left ventro-caudal lobe (Tween-injured tissue) were excised; one segment of each tissue type was submerged in formalin for histopathologic analysis, and another segment of each was snap frozen in liquid nitrogen. Normal saline (60 mL) was instilled separately into the right middle lobe (non-Tween-injured tissue) and the right dorso-caudal lobe (Tween-injured tissue) to collect BALF. The BALF was spun (Beckman Coulter Allegra X-22R Centrifuge, Indianapolis, IN; 3,000 rpm for 10 min at 4°C) and the supernatant snap frozen. The resulting pellet was resuspended and 200 μL of the sample was spun using a cytopath device (Zentrifugen Hettich Rotofix 32 A, Tuttlingen, Germany; 1,000 rpm for 3 min at room temperature) onto a cytology funnel (BMP Biomedical Polymers, Sterling, MA) to create a cytopath slide. The cytopath slide was stained using hematoxylin and

eosin and analyzed under light microscopy ($\times 1,000$ magnification and oil immersion). One hundred cells were analyzed for inflammatory cell identification. The investigators performing the cytopath analysis (BR and JV) were blinded to the treatment groups and samples.

The lung tissue fixed in formalin was sent to HistoWiz Inc. (Brooklyn, NY) for staining with standard hematoxylin and eosin staining. The quantitative histological assessment of the lung was based on the image analysis of 800 photomicrographs (10 apical and 10 basilar) made at high-dry magnification following a validated, unbiased, systematic sampling protocol (25). Each photomicrograph was scored using a 4-point scale for each of three parameters: fibrinous deposits, blood in air space, and leukocytes. The investigator performing the histologic analysis (LAG) was blinded to the treatment groups and samples.

Fresh lung tissue, collected from the right and left apical and basilar lobes was minced and weighed to determine the “wet” weight. The tissue was then placed into an oven set to 60°C and weighed daily until there was no change in weight for two consecutive days to determine the “dry” weight. The wet-to-dry ratio was then calculated using the formula (wet – dish weight)/(dry – dish weight).

Statistical Analysis

Descriptive statistics are reported as mean and standard error. A repeated measures ANOVA test was used to compute differences within and between treatment groups. Post hoc Tukey’s tests were performed on continuous data at multiple time points for significance found during repeated measures ANOVA testing. Student’s *t* tests were also performed to assess differences between groups. $P < 0.05$ was considered statistically significant. Statistical analysis was performed using Prism 9 (Graphpad Software, CA) and Origin (OriginLab Corp., Northampton, MA).

RESULTS

Hemodynamics

Heart rate, cardiac output, and global end-diastolic volume were similar among groups (Table 1). Total resuscitation fluid volume was higher and net fluid balance more positive in $OD \uparrow RD \downarrow$ compared with all other groups and were associated with a more negative absolute base excess. Hourly urine output was similar among groups (between 2.2 and 2.8 mL/kg/h by the 6 h study end). Animals with $OD \downarrow$ had a trend toward higher MAP but the effect diminished by the end of the study and was not significant. Animals with $OD \downarrow$ did not require vasopressors to maintain MAP, whereas animals with $OD \uparrow$ did. Of the $OD \uparrow RD \downarrow$ group, 7 animals required norepinephrine (average 2.8 h; median 2 h after injury) and 4 of the $OD \uparrow RD \uparrow$ group required norepinephrine (average 3.3 h; median 3.5 h after injury).

Pulmonary Function

Figure 3, A–D shows how respiratory function behaved for each of the four groups of pigs before and following lung injury. Figure 3A demonstrates that in the absence of both OD and RD ($OD \downarrow RD \downarrow$), $\text{Pa}_{\text{O}_2}/\text{Fl}_{\text{O}_2}$ rebounds quickly above clinical ARDS values ($\text{Pa}_{\text{O}_2}/\text{Fl}_{\text{O}_2} < 300$ mmHg) shown as the

Table 1. Cardiac and fluid parameters at baseline (following injury) and at 0, 3, and 6 h of mechanical ventilation with higher or lower levels of overdistension and recruitment/derecruitment

	Groups	BL	T0	T3	T6	P Value
Heart rate, beats/min	OD↓RD↓	92.6±5.2	104.1±9.1	90.4±6.2	97.5±10.7	0.14
	OD↓RD↑	90.8±5.3	104.8±4.3	95.8±8.5	87.2±5.9	
	OD↑RD↓	90.2±4.6	114.8±7.4	121.4±10.1	118.3±11.4	
	OD↑RD↑	98.2±9.4	122.6±10	102.8±7.5	93.2±8.2	
Mean arterial pressure, mmHg	OD↓RD↓	128.6±4.7	108±5.0	80.6±4.1§	71.9±4.0	0.10
	OD↓RD↑	132.6±5.4	107.7±4.3	98.7±3.2*	81.3±3.6	
	OD↑RD↓	123.5±4.0	98.1±6.0	77.7±4.9§	69.2±6.1	
	OD↑RD↑	126.9±3.2	99.6±5.1	71.8±2.9§	73.5±4.4	
Cardiac output, L/min	OD↓RD↓	4.9±0.4	3.3±0.2	2.8±0.2	2.5±0.3	0.30
	OD↓RD↑	4.6±0.5	4.1±0.4	2.5±0.2	2.7±0.3	
	OD↑RD↓	5.0±0.4	2.9±0.3	2.4±0.2	2.0±0.2	
	OD↑RD↑	5.3±0.6	3.5±0.4	2.5±0.2	2.8±0.3	
Global end-diastolic volume, mL	OD↓RD↓	618.3±26.4	596.4±36.0	540.6±16.8	496.6±34.9	0.21
	OD↓RD↑	640.8±41.5	608.7±47.6	515.0±39.7	539.8±32.9	
	OD↑RD↓	674.2±41.9	555.3±27.3	502.6±39.4	461.7±32.3	
	OD↑RD↑	640.1±30.8	551.2±38.2	519.6±23.8	548.4±40.5	
Extravascular lung water index	OD↓RD↓	8.1±0.3	8.5±0.3	8.3±0.5‡	8.3±0.3‡	<0.0001
	OD↓RD↑	9.0±0.5	10.0±0.5	10.8±1.2	9.6±0.7‡	
	OD↑RD↓	8.4±1.0	9.0±0.6	10.6±1.1	9.5±0.9‡	
	OD↑RD↑	8.0±0.3	9.9±0.5	14.1±1.0&	13.2±0.9*	
Pulmonary vascular permeability index	OD↓RD↓	2.6±0.1	2.9±0.2	3.1±0.2‡	3.6±0.2‡	0.0002
	OD↓RD↑	2.9±0.2	3.4±0.3	3.9±0.3‡	3.7±0.4	
	OD↑RD↓	2.5±0.2	3.3±0.2	4.4±0.3&	4.5±0.5	
	OD↑RD↑	2.5±0.1	3.9±0.4	5.6±0.4&	5.0±0.3&	
Total fluids in, L	OD↓RD↓	1.6±0.2	2.5±0.1	4.3±0.3†	6.3±0.4†	<0.0001
	OD↓RD↑	1.8±0.2	2.6±0.0	3.5±0.1†	5.3±0.4†	
	OD↑RD↓	1.7±0.2	2.4±0.3	6.1±0.4*	10.1±0.5*	
	OD↑RD↑	1.7±0.2	2.8±0.2	4.5±0.4†	6.7±0.6†	
Hourly urine output, mL/kg	OD↓RD↓	10.8±2.3	3.1±0.7	2.9±0.5	2.2±0.5	0.40
	OD↓RD↑	7.9±2.0	2.7±0.5	2.4±0.5	2.2±0.7	
	OD↑RD↓	5.1±0.8	3.1±0.8	2.5±0.6	2.8±0.6	
	OD↑RD↑	9.5±2.2	4.1±1.5	2.8±0.9	2.4±0.6	
Net fluid balance, L	OD↓RD↓	1.2±0.3	1.9±0.2	3.4±0.3†	5.0±0.4†	<0.0001
	OD↓RD↑	1.5±0.1	2.2±0.1	2.8±0.1†	4.2±0.3†	
	OD↑RD↓	1.4±0.2	2.1±0.3	5.5±0.4*	9.3±0.5*	
	OD↑RD↑	1.2±0.2	2.3±0.2	3.7±0.4†	5.5±0.6†	
Pa _{CO₂} , mmHg	OD↓RD↓	39.8±0.6	43.7±1.1	33.9±1.8*	28.7±1.7	0.0074
	OD↓RD↑	41.8±1.4	45.4±1.6	25.6±1&	23.6±1.1	
	OD↑RD↓	41.1±1.2	43.8±1.8	25.2±1&	21.9±1.7	
	OD↑RD↑	42.8±1.1	44.8±1.1	22±2&	24.3±3.2	
Base excess	OD↓RD↓	3.3±0.5	2.8±0.6	-2.7±0.8	-3.8±1.1†	0.0023
	OD↓RD↑	3.5±0.4	3.3±0.4	-1.7±0.9‡	-2.8±1.4†	
	OD↑RD↓	3.1±0.6	2.5±0.8	-5.7±0.9§	-8.4±1.0&§	
	OD↑RD↑	2.8±0.5	2.0±0.5	-5.7±1.0§	-6.7±1.2	
pH	OD↓RD↓	7.46±0.01	7.42±0.01	7.42±0.02§†	7.43±0.03	<0.0001
	OD↓RD↑	7.44±0.01	7.41±0.01	7.51±0.02&	7.52±0.02	
	OD↑RD↓	7.44±0.01	7.41±0.01	7.46±0.02‡	7.44±0.04	
	OD↑RD↑	7.43±0.01	7.40±0.01	7.49±0.03&†	7.44±0.03	

&P < 0.05 vs. OD↓RD↓; §P < 0.05 vs. OD↓RD↑; †P < 0.05 vs. OD↑RD↓; ‡P < 0.05 vs. OD↑RD↑; *P < 0.05 vs. all groups. BL, baseline; OD, overdistension; Pa_{CO₂}, arterial partial pressure of carbon dioxide; recruitment/derecruitment; ↑, higher levels; ↓, lower levels.

pink region in Fig. 3A) following injury. A slightly reduced degree of recovery is seen with OD alone (OD↑RD↓). In contrast, both groups with RD (OD↑RD↑ and OD↓RD↑) had markedly suppressed recoveries; both RD and OD together (OD↑RD↑) met the clinical definition of ARDS over the entire time-course of the experiment, whereas with RD alone (OD↓RD↑), the lungs showed signs of recovery after ~3 h. Figure 3B shows Pa_{O₂}/Fi_{O₂} relative to 300 mmHg averaged over T0 to T6 for each of the four groups. This is essentially equivalent to the areas, either above or below the pink region in Fig. 3A, of the time profiles shown in Fig. 3A. The P values between group averages (two-sample *t* test) are also shown in Fig. 3B. As suggested by visual inspection of Fig. 3A, Fig. 3B shows that all comparisons reach statistical significance

at *P* < 0.05, but that these differences are much stronger between groups that differ in RD as opposed to OD.

The temporal patterns in Pa_{O₂}/Fi_{O₂} are largely mirrored by those in *nC_{rs}* (Fig. 3C), although with a clearer distinction between the groups with RD versus those with OD. The average values of *nC_{rs}* relative to 1.0 (ΔnC_{rs}) from T0 to T6 (Fig. 3D) demonstrate highly significant differences between groups with and without RD, but nonsignificant differences between groups with and without OD. The results in Fig. 3 thus demonstrate that lung injury recovered most quickly in the absence of both OD and RD (OD↓RD↓) and most deficient when both were present (OD↑RD↑). Importantly, OD alone (OD↑RD↓) resulted in better recovery than RD alone (OD↓RD↑).

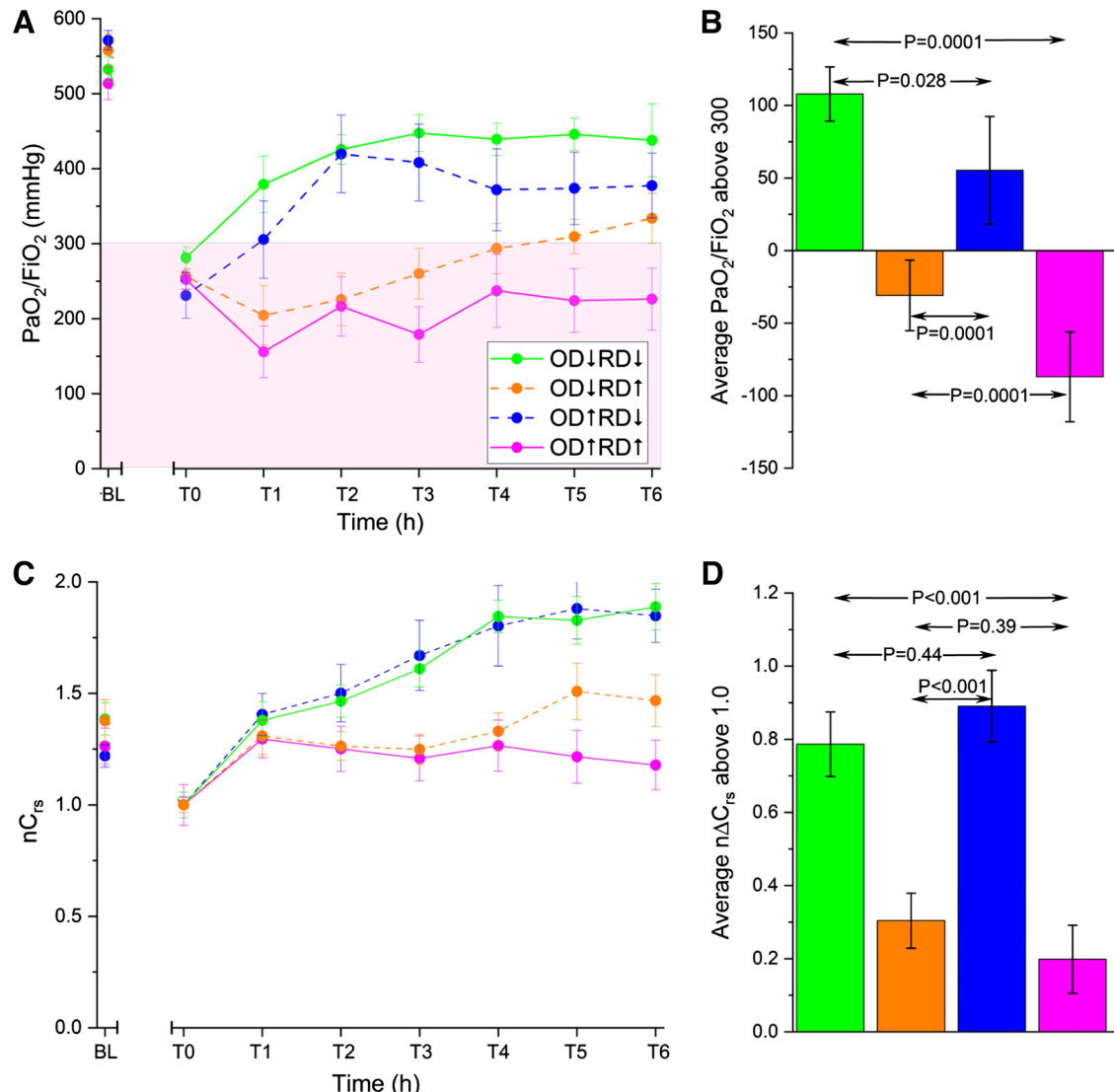


Figure 3. Pulmonary function parameters from groups ($n=10$ pigs per group) with higher (\uparrow) or lower (\downarrow) overdistension (OD) and recruitment/derecruitment (RD). Ratio of arterial oxygen partial pressure (PaO_2) to fraction of inspired oxygen (FiO_2) over the course of the experiment (A), average mean values of $\text{PaO}_2/\text{FiO}_2$ from T_0 to T_6 relative to a value of 300 mmHg (B), respiratory system compliance, measured by the forced oscillation technique, normalized to its value immediately postinjury (nC_{rs} ; C), and average mean values of respiratory system compliance relative to the postinjury value of 1.0 (D). Measurements were obtained at b prior to injury (BL) and for 6 h following lung injury (T_0-T_6). Data represented as means \pm SE. P values determined from two-sample t tests between the indicated groups.

Figure 4 shows how OD and RD affected ΔP and V_T . The group differences between these two parameters are in marked contradistinction to the differences in $\text{PaO}_2/\text{FiO}_2$ and nC_{rs} shown in Fig. 3. Specifically, although ΔP and V_T were again very different between $\text{OD} \uparrow \text{RD} \uparrow$ and $\text{OD} \downarrow \text{RD} \downarrow$ (highly significant P values in Fig. 4, B and D), there were no differences between the groups with OD alone versus RD alone for either parameter. In other words, we found a dissociation between how OD versus RD affected $\text{PaO}_2/\text{FiO}_2$ and nC_{rs} , both markers of VILI, compared with how they affected ΔP and V_T , both indicators of the interaction between ventilator and lung.

Figure 5A provides the post injury time-courses of PEEP and T_{Low} , two additional parameters of ventilator-lung interaction. PEEP in this case is the airway pressure that pertained at the termination of expiration, so as expected it was higher in the two $\text{RD} \downarrow$ groups, in which expiration was

terminated, early compared with the two $\text{RD} \uparrow$ groups (Fig. 5A). For the same reason, T_{Low} was also lower in the two $\text{RD} \downarrow$ groups. The rank ordering of the four groups, as well as their clustering, was different between PEEP and T_{Low} .

Because of our study design, T_{High} was the same among the four groups and occupied the vast majority of the ventilator cycle. Consequently, there were no significant differences in respiratory rate despite the adjustments in T_{Low} . The respiratory rate at T_6 in $\text{OD} \downarrow \text{RD} \downarrow$ was 13.5 ± 0.2 breaths/min, as compared with 13.8 ± 1.1 breaths/min in $\text{OD} \downarrow \text{RD} \uparrow$, 13.8 ± 0.5 breaths/min in $\text{OD} \uparrow \text{RD} \downarrow$, and 13.0 ± 1.9 breaths/min in $\text{OD} \uparrow \text{RD} \uparrow$.

Injury Biomarkers

Figure 6 and Table 1 provide biomarkers for each of the groups. There was no difference between groups in the Wet/

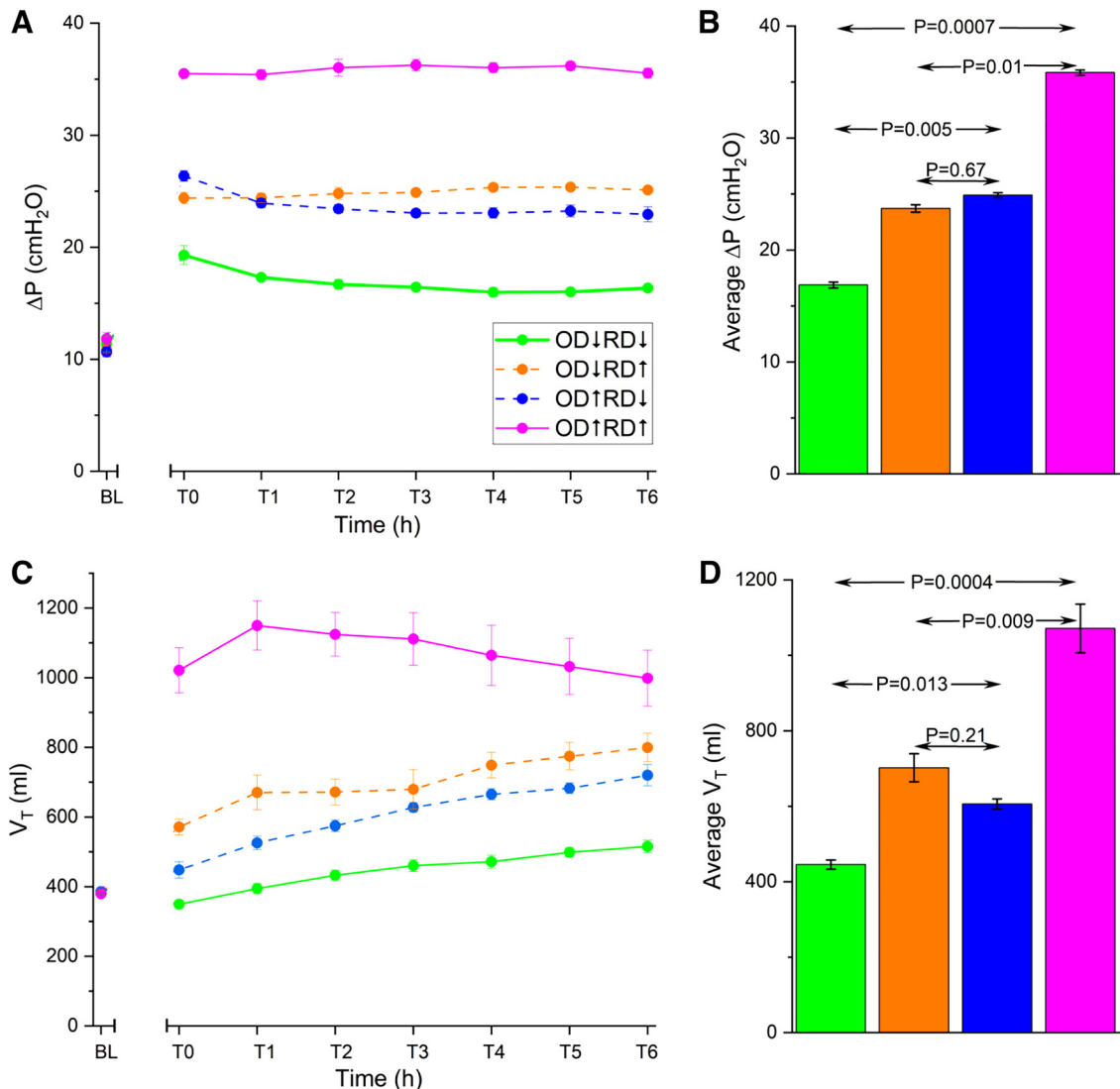


Figure 4. Mechanical ventilation system behavior for each group ($n = 10$ pigs per group) with higher (\uparrow) or lower (\downarrow) overdistension (OD) and recruitment/derecruitment (RD). Driving pressure (ΔP) over the course of the experiment calculated as the difference between plateau and positive end-expiratory pressures (A), average ΔP from T0 to T6 (B), tidal volume (V_T ; C), and average V_T from T0 to T6 for each group (D). Parameters were recorded at baseline (BL, before lung injury) and following lung injury for 6 h (T0–T6). Data represented as means \pm SE. P values determined from two-sample t tests between the indicated groups.

Dry lung weight ratio in the normal tissue from the apical lung (Fig. 6A). However, OD \uparrow groups had increased ratios of wet/dry lung weight compared with OD \downarrow groups in the surfactant dysfunctional tissue from the basilar regions of the lung (Fig. 6A). Total Protein in the BALF was not different between groups in the normal tissue (Fig. 6B) but was significantly increased in the surfactant dysfunctional tissue of OD \uparrow RD \uparrow (Fig. 6B). The neutrophil count in the BALF was elevated in both normal and surfactant dysfunctional tissue of OD \uparrow RD \uparrow (Fig. 6C), whereas the macrophage count was lower (Fig. 6D). OD \uparrow RD \uparrow had increased extra vascular lung water compared with the other three groups, and an elevated pulmonary vascular permeability index compared with OD \downarrow RD \downarrow (Table 1).

Figure 7 provides histological evidence for each of the groups. Normal tissue from the lung apices showed less histological evidence of injury than the surfactant dysfunctional tissue from the lung bases (Fig. 7, A–D).

Histopathologic injury in the form of elevated red and white blood cells was only seen in the normal tissue in OD \uparrow RD \uparrow (Fig. 7D). In the surfactant dysfunctional tissue, the white blood cell count was elevated in OD \uparrow RD \uparrow compared with the other three groups, whereas the red blood cell count was greater in OD \uparrow RD \uparrow compared with either OD \downarrow RD \downarrow or OD \downarrow RD \uparrow (Fig. 7D). The amount of fibrin in the airways was greater in OD \uparrow RD \uparrow compared with OD \downarrow RD \uparrow or OD \uparrow RD \downarrow but not OD \downarrow RD \downarrow (Fig. 7D).

DISCUSSION

Minimizing VILI is critical to the management of ARDS, a devastating lung injury characterized by heterogeneous pulmonary edema leading to surfactant dysfunction and widespread collapse of the pulmonary airspaces (1). It is well accepted that two key mechanical drivers of VILI are OD (which leads to volutrauma) and RD (which leads to

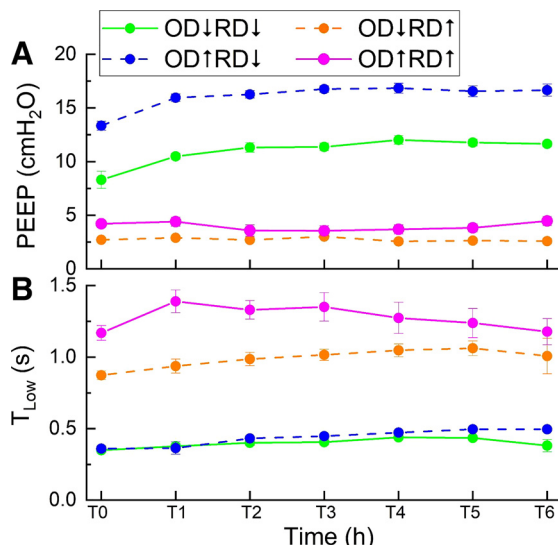


Figure 5. Additional mechanical ventilation system behavior for each group ($n = 10$ pigs per group) with higher (\uparrow) or lower (\downarrow) overdistension (OD) and recruitment/derecruitment (RD). Positive end-expiratory pressure (PEEP; A) and duration of expiration (T_{low} ; B). Parameters were recorded following lung injury for 6 h (T_0 – T_6). Data are means \pm SE.

atelectrauma) (26). Although these two forms of injury are generally presumed to result from independent mechanisms that manifest during mechanical ventilation at high and low lung volumes, respectively, their ranges of action can overlap significantly in the injured lung (11). Data from mouse models further suggest that coincident volutrauma and atelectrauma act synergistically (5) to cause an accelerating permeability-originated obstructive response (POOR) (26) in which the blood-gas barrier compromise created by RD becomes progressively worsened by OD (27, 28). Nevertheless, the relative roles of OD and RD in VILI remain unclear.

Elucidating the roles of OD and RD in VILI is complicated by the fact that neither injury mechanism can be neither entirely abrogated, nor controlled with complete independence, by any mechanical ventilation strategy. The APRV mode, however, does permit some degree of independent control of OD (through the parameter P_{High}) versus RD (through the parameter T_{Low}). V_T and ΔP , in contrast, are not controlled during APRV because they are consequences of T_{High} , P_{High} , T_{Low} , and P_{Low} acting on the mechanics of a particular lung. By the same token, this highlights the importance of making sure that minute ventilation during APRV is sufficient to meet the gas exchange needs of the patient. Monitoring O_2 saturation and/or end-tidal CO_2 may thus be particularly important during this mode of mechanical ventilation.

Our data demonstrate that VILI is caused either by a large maximum stretch imposed on the lung tissues (i.e., OD alone with a P_{High} of 40 cmH₂O) or by the RD that results from an extended T_{Low} . It is clear from Fig. 3 that VILI is especially pronounced when both OD and RD are present simultaneously. These findings are supported by a picture of increased airway protein and cellularity consistent with tissue inflammation (Fig. 6), and postmortem histology typical of the deceased patient with ARDS (Fig. 7). Figure 3 also suggests that RD alone (OD↓RD↑) is more damaging to respiratory

function than OD alone (OD↑RD↓), which corroborates other studies (29). On the other hand, the biomarker findings (Fig. 6) suggest that OD alone is at least as damaging as RD alone. There may thus be some degree of disconnect between biomarkers of injury and its clinical manifestations, for reasons that remain to be elucidated.

Importantly, V_T and ΔP do not move in lock step with the APRV parameters, which allows us to infer something about the importance of these parameters for the production of VILI. In this regard, perhaps the most important finding of our study is that V_T and ΔP (Fig. 4, A–D) are dissociated from the physiological VILI markers Pao_2/FiO_2 and nC_{rs} (Fig. 3, A–D). Specifically, even after Bonferroni correction for multiple comparisons, there is no difference in either V_T or ΔP when only OD or RD is present (OD↑RD↓ or OD↓RD↑; Fig. 4, B and D), whereas there are significant differences in Pao_2/FiO_2 and nC_{rs} in either case (Fig. 3, B and D). These findings thus suggest that, contrary to conventional thinking, VILI is not reduced during APRV by employing a low V_T .

Teasing apart the intermediate cases (OD↑RD↓ vs. OD↓RD↑) with respect to the mechanical stimuli (beyond V_T or ΔP) is particularly insightful because it can causally inform us of the stimulus that is most likely to lead to VILI. The present studies indicate that protection is afforded by short-duration exhalation (small T_{low}) since this provides less time for derecruitment (Fig. 5B). This is illustrated best by the intermediate cases (OD↑RD↓ or OD↓RD↑), where better respiratory function exists for OD↑RD↓ even though there is no difference in V_T or ΔP . Unfortunately, this causality is not straight-forward, as low T_{low} is also associated with high effective PEEP (Fig. 5A). It should be noted, however, that the most protective strategy, namely OD↓RD↓, has an effective PEEP that is substantially lower than OD↑RD↓, so higher PEEP itself is not necessarily protective. Clearly, exhalation timing (T_{low}) is a critically important independent parameter that aligns with protection from VILI through the reduction of RD.

These results are consistent with our previous findings in rodents using intravital microscopy showing direct visual evidence of RD occurring at the alveolar level with no obvious OD (30). Other studies have also shown that RD causes more VILI than OD. For example, Seah et al. (5) found that RD is necessary to induce VILI in normal mice. Protti et al. (31) demonstrated that static strain with PEEP as high as 19 cmH₂O was less likely to lead to pulmonary edema than dynamic strain (31). Tremblay et al. (32) showed in mice that PEEP of 0 cmH₂O resulted in significantly higher levels of lung inflammation, as measured by TNF- α and IL-1 β , compared with PEEP of 10 cmH₂O. Otto et al. (33) studied the cyclic RD in dependent lung regions and OD in nondependent lung regions in rabbits with surfactant deactivation ventilated with supraphysiologic V_T (28 mL/kg) and low PEEP (2 cmH₂O), and determined that cyclic RD was associated with greater inflammatory injury compared with OD (33). Using a porcine lung injury model similar to that of the present study, Jain et al. (21) showed that ventilation with low effective PEEP (produced by a longer expiratory duration) resulted in significantly more histologic injury and pulmonary edema compared with high PEEP (produced by a much shorter expiratory

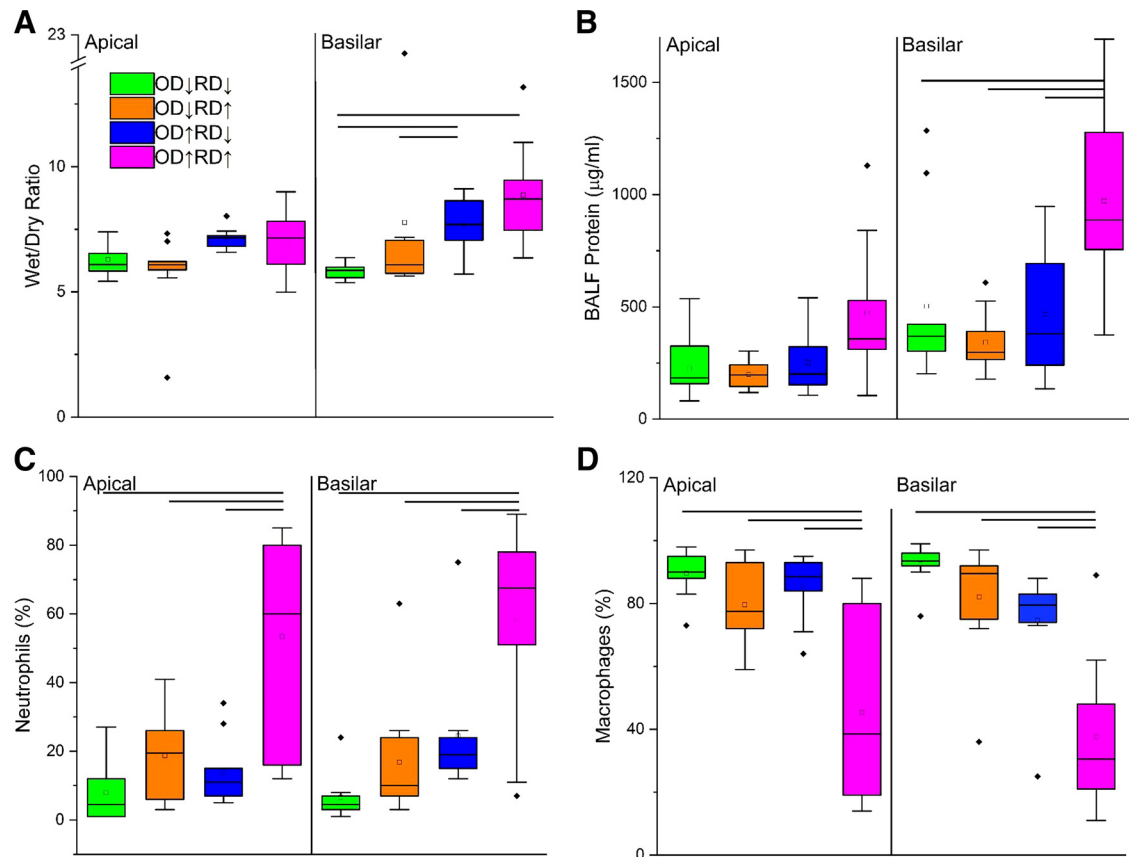


Figure 6. Lung edema assessed as a lung tissue wet to dry weight ratio (wet/dry ratio; *A*), total protein in bronchoalveolar lavage fluid (BALF; *B*), neutrophil counts (*C*), and macrophage counts measured using Cytopsin (*D*). Groups ($n = 10$ pigs per group) were ventilated with a combination of higher (\uparrow) or lower (\downarrow) overdistension (OD) and recruitment/derecruitment (RD). Measurements were made in both normal (apical) and surfactant dysfunctional (basal) tissues. Black dots indicate outliers. Horizontal lines represent $P < 0.05$ between groups (ANOVA).

duration) despite a high plateau pressure (P_{plat}) of 40 cmH₂O, similar to results of the present study (21). These various findings, together with those of the present study, point to a preeminent role for RD in the pathogenesis of VILI. On the other hand, Mertens et al. (34) observed the occurrence of alveolar distension rather than RD, which may reflect the fact that intravital microscopy is a challenging technique requiring sub-pleural alveoli be controlled by suction to a glass slide.

Because we targeted Tween-induced surfactant injury to the basilar regions of the lung, leaving the apical regions essentially normal, we can see that the VILI caused by OD and RD together in these respective lung regions depends on the existing injury status of the lung tissue (Figs. 6 and 7). This supports the notion put forward by Seah et al. (5) that one can view a given regimen of conventional mechanical ventilation as a point in the V_T /PEEP plane. This plane consists of two distinct regions: 1) a safe region in which VILI does not occur and 2) a damaging region within which VILI progresses. It was also proposed that the safe region in the V_T /PEEP plane shrinks progressively as tissue injury worsens such that there may come a point at which there is no physiologically sustainable combination of V_T and PEEP that is safe. This view of VILI progression is similar to the “VILI Vortex” envisioned by Marini and Gattinoni (35) in which progressive loss of functional

residual capacity (FRC) creates a so-called baby lung that becomes increasingly susceptible to OD injury.

Our findings have significant implications for the clinical management of the patient with ARDS, which is currently dominated by the use of low V_T (LV_T) ventilation as a result of the ARDSnet clinical trial in 2000 (10). The rationale for LV_T ventilation is that a certain fraction of the ARDS lung is collapsed and cannot be ventilated, so using a reduced V_T prevents OD of the remainder (the ‘baby lung’ argument). In a subsequent analysis, however, Amato et al. (36) showed that improved outcomes were obtained by using ΔP (V_T normalized to C_{rs}) to guide ventilation. This was supported by a retrospective analysis of patients in prior randomized controlled trials by Guerin et al. (37) who showed that ΔP was 13.7 ± 3.7 cmH₂O in ARDS nonsurvivors compared with 12.8 ± 3.7 cmH₂O in survivors. These studies confirm the intuitively obvious notion that a one-size-fits-all V_T strategy in ARDS cannot be optimal for all patients (38). Indeed, even when smaller V_T are used, patients may still be at risk for volutrauma if lung C_{rs} is sufficiently low (39). To counter this, P_{plat} is often used as a surrogate for OD (10). There is some suggestion, however, that strict adherence to the ARDSnet strategy of $P_{plat} < 30$ cmH₂O could cause further harm if the patient characteristics and ARDS phenotype are not taken into consideration (40). Conversely,

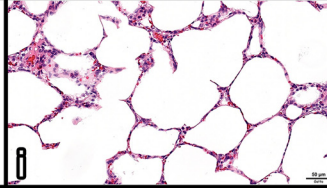
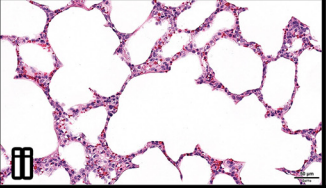
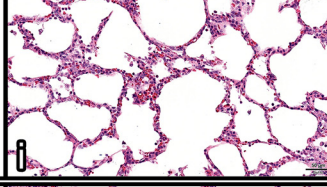
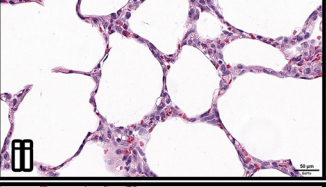
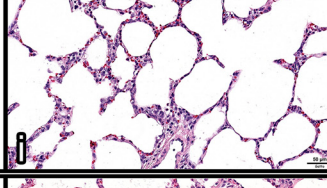
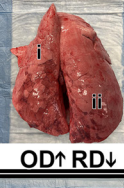
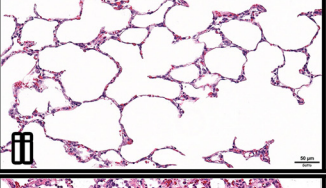
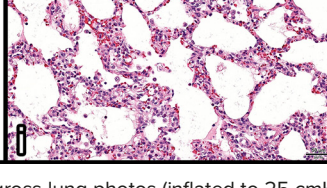
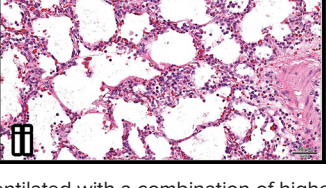
Apical Scoring	Apical Histology (non-tween)	Whole Lung	Diaphragmatic Histology (tween-injured)	Diaphragmatic Scoring
Fibrin 0.87 ± 0.18 RBC 0.20 ± 0.31 WBC 0.10 ± 0.06		 OD↓ RD↓		Fibrin 1.42 ± 0.33 RBC 0.33 ± 0.20 WBC $0.15 \pm 0.12^{\ddagger}$
Fibrin 1.02 ± 0.15 RBC 0.22 ± 0.10 WBC 0.17 ± 0.08		 OD↓ RD↑		Fibrin $1.11 \pm 0.15^{\ddagger}$ RBC 0.36 ± 0.14 WBC $0.30 \pm 0.10^{\ddagger}$
Fibrin 0.69 ± 0.12 RBC 0.41 ± 0.15 WBC 0.19 ± 0.09		 OD↑ RD↓		Fibrin $1.02 \pm 0.18^{\ddagger}$ RBC 0.42 ± 0.12 WBC 0.46 ± 0.12
Fibrin 0.96 ± 0.22 RBC 1.00 ± 0.32 WBC 1.05 ± 0.34		 OD↑ RD↑		Fibrin $1.87 \pm 0.20^{\ddagger\$}$ RBC 1.13 ± 0.28 WBC $1.39 \pm 0.31^{\ddagger\$}$

Figure 7. Histopathology and gross lung photos (inflated to 25 cmH₂O) in groups ventilated with a combination of higher (↑) or lower (↓) overdistension (OD) and recruitment/derecruitment (RD). Measurements were made in both normal (apical) and surfactant dysfunctional (basal) tissues. Fibrin, red blood cells (RBC), and white blood cells (WBC) in the airway were quantitatively analyzed. Data means \pm SE. $^{\ddagger}P < 0.05$ vs. OD↑RD↓; $^{\ddagger}P < 0.05$ vs. OD↑RD↑; $^{\ddagger}P < 0.05$ vs. OD↓RD↑; $^{\ddagger}P < 0.05$ vs. OD↓RD↓; $^{\ddagger}P < 0.05$ vs. OD↑RD↓. $n = 10$ pigs per group.

patients with reduced chest wall compliance due to obesity (41) or extrapulmonary ARDS (40, 42) benefit from ventilation with a Pplat >30 cmH₂O.

RD can be significantly modulated by the magnitude of intratidal excursions in lung volume, particularly when lung volume changes take place over the lower end of the volume range where inflation pressures are too low to prevent regional collapse. Although PEEP has been widely advocated as a method of preventing such collapse (43), PEEP alone is not necessarily the answer, nor is it synonymous with lung recruitability (44). It may be impossible to ventilate the injured lung above the volume range over which RD occurs (11), which could explain in part why Protti et al. (31) found that increased levels of dynamic strain but not static strain resulted in significant accrual of pulmonary edema. Our study supports these findings since OD alone (OD↑RD↓) maintained a higher nC_{rs} , a higher and rapidly improving Pa_{O_2}/Fi_{O_2} , than RD alone (OD↓RD↑; Fig. 3).

The above discussion might seem to indicate that ventilating the injured lung with a small V_T would be a reasonable strategy to minimize damaging intratidal RD. Unfortunately, this is problematic because pathophysiologic tissue stresses are often concentrated in the parenchymal tissues lying at the interface between open and closed lung compartments (45). These regions have been termed stress multipliers (46, 47) and result in increased dynamic tissue strain even

when V_T is low (48). Avoiding this situation requires recruiting atelectatic lung regions, something that is often challenging clinically and may require the persistent application of elevated pressure. Here, APRV has an advantage in that it exposes the lung to a higher airway pressure (P_{High}) for the vast majority of the breath cycle (T_{High}), effectively creating continuous positive airway pressure (CPAP). Using APRV, it may take hours or even days to fully open the lung in cases of severe injury (49), again highlighting the fact that pressure alone is not the only consideration when it comes to ventilating the injured lung; time is also critically important. Regardless of its apparent benefits, however, APRV comes with an important caveat. Although an appropriately small value of T_{Low} can greatly abrogate RD, increasing T_{Low} above this value by even a small amount, often less than a second, can allow enough time for excessive RD to occur. This can have disastrous consequences for the lung, as our present findings demonstrate. To be effective, therefore, APRV must be applied with precision, something that requires special attention in a clinical setting. Furthermore, continual monitoring is required so that T_{Low} can be adjusted to account for any changes that might occur in C_{rs} as the condition of a patient changes (50).

Our study has several limitations. First, we used high airway pressures to generate OD and long expiratory durations to facilitate lung collapse. These ventilator settings are not

relevant to clinical application of APRV; they were chosen specifically to produce VILI to gain insight into injury mechanisms. Second, although surfactant deactivation produced by Tween instillation recapitulates a primary pathophysiology associated with ARDS (1), it does not encompass the inflammatory injury associated with pneumonia or extrapulmonary lung injury. Third, our study was conducted over only 6 h, which is brief compared with the time spent on mechanical ventilation by many APRV patients. Our results must be viewed as relevant to the acute mitigation of VILI and not its long-term sequelae. Finally, we only examined APRV in the present study so did not, for example, compare it to conventional ventilation strategies such as the LT_V approach. Such a comparison would certainly be valuable but is complicated by the fact that V_T , ΔP , and effective PEEP cannot all be simultaneously identical when using conventional ventilation versus APRV. A comprehensive comparison of the two ventilation modes would thus be a major undertaking that goes beyond the scope of the present study. Nevertheless, the relative advantages of APRV versus LT_V remains an important topic for future investigation.

In conclusion, OD and RD are both capable of causing VILI in the injured lung, but our study shows in a porcine model of ARDS that, of these two phenomena, avoiding RD is the preeminent consideration. To arrive at these conclusions, we exploited the fact that APRV allows for the independent adjustment of the temporal and amplitude aspects of the ventilatory pressure waveform. However, although our results show that APRV can be very protective for the lung when applied with the appropriate values of its four defining parameters P_{High} , T_{High} , P_{Low} and T_{Low} , substantial VILI results if inappropriate values of P_{High} and especially T_{Low} are used. These findings demonstrate that considerations of time can be as important as pressure for safely ventilating the injured lung and suggest that timing should be taken into account when managing patients with ARDS.

GRANTS

This work was supported by NIH Grant R01HL142702 and by W81XWH2010696 (US Army MEDCOM Congressionally Directed Medical Research Programs).

DISCLAIMERS

The authors maintain that industry had no role in the design and conduct of the study; the collection, management, analysis, or interpretation of the data; nor the preparation, review, or approval of the manuscript.

DISCLOSURES

J.H.T.B is a member of the advisory board and shareholder in Oscillavent, LLC. He is also a consultant for Respirator Sciences LLC. G.F.N. and M.K-S. have lectured for Intensive Care On-line Network, Inc. (ICON). N.M.H. is the founder of ICON, of which P.L.A. is an employee. N.M.H. holds patents on a method of initiating, managing, and/or weaning airway pressure release ventilation, as well as controlling a ventilator in accordance with the same. M.K-S. has received an educational research grant from Dräger Medical Systems, Inc.

AUTHOR CONTRIBUTIONS

J.H.T.B., D.P.G., and G.F.N. conceived and designed research; H.R., J.S. and S.B. performed experiments; J.H.T.B., J.S., D.P.G., L.A.G., A.J.G., H.R., B.R., J.V., N.M.H., N.D., M.K-S., and G.F.N. analyzed data; J.H.T.B., J.S., P.L.A., D.P.G., G.W., A.J.G., N.M.H., N.D., M.K-S., and G.F.N. interpreted results of experiments; H.R., J.H.T.B., J.S., and A.J.G. prepared figures; H.R. drafted manuscript; H.R., B.R., J.V., N.M.H., N.D., M.K-S., G.F.N., J.H.T.B., J.S., S.B., P.L.A., D.P.G., L.A.G., G.W., and A.J.G. edited and revised manuscript; H.R., J.H.T.B., J.S., S.B., P.L.A., D.P.G., L.A.G., G.W., A.J.G., B.R., J.V., N.M.H., N.D., M.K-S., and G.F.N. approved final version of manuscript.

REFERENCES

- Matthay MA, Zemans RL, Zimmerman GA, Arabi YM, Beitler JR, Mercat A, Herridge M, Randolph AG, Calfee CS. Acute respiratory distress syndrome. *Nat Rev Dis Primers* 5: 18, 2019. doi:10.1038/s41572-019-0069-0.
- Bellani G, Laffey JG, Pham T, Fan E, Brochard L, Esteban A, Gattinoni L, van Haren F, Larsson A, McAuley DF, Ranieri M, Rubenfeld G, Thompson BT, Wrigge H, Slutsky AS, Pesenti A; LUNG SAFE Investigators, ESICM Trials Group. Epidemiology, patterns of care, and mortality for patients with acute respiratory distress syndrome in intensive care units in 50 countries. *JAMA* 315: 788–800, 2016. doi:10.1001/jama.2016.0291.
- Protti A, Andreis DT, Iapichino GE, Monti M, Comini B, Milesi M, Zani L, Gatti S, Lombardi L, Gattinoni L. High positive end-expiratory pressure: only a dam against oedema formation? *Crit Care* 17: R131, 2013. doi:10.1186/cc12810.
- Wilson MR, Patel BV, Takata M. Ventilation with “clinically relevant” high tidal volumes does not promote stretch-induced injury in the lungs of healthy mice. *Critical Care Med* 40: 2850–2857, 2012. doi:10.1097/CCM.0b013e31825b91ef.
- Seah AS, Grant KA, Aliyeva M, Allen GB, Bates JHT. Quantifying the roles of tidal volume and PEEP in the pathogenesis of ventilator-induced lung injury. *Ann Biomed Eng* 39: 1505–1516, 2011. doi:10.1007/s10439-010-0237-6.
- Bilek AM, Dee KC, Gaver DP 3rd. Mechanisms of surface-tension-induced epithelial cell damage in a model of pulmonary airway reopening. *J Appl Physiol (1985)* 94: 770–783, 2003. doi:10.1152/japplphysiol.00764.2002.
- Kay SS, Bilek AM, Dee KC, Gaver DP 3rd. Pressure gradient, not exposure duration, determines the extent of epithelial cell damage in a model of pulmonary airway reopening. *J Appl Physiol (1985)* 97: 269–276, 2004. doi:10.1152/japplphysiol.01288.2003.
- Yamaguchi E, Yao J, Aymond A, Chrisey DB, Nieman GF, Bates JHT, Gaver DP. Electric cell-substrate impedance sensing (ECIS) as a platform for evaluating barrier-function susceptibility and damage from pulmonary atelectrauma. *Biosensors (Basel)* 12: 390, 2022. doi:10.3390/bios12060390.
- Jacob AM, Gaver DP 3rd. Atelectrauma disrupts pulmonary epithelial barrier integrity and alters the distribution of tight junction proteins ZO-1 and claudin 4. *J Appl Physiol (1985)* 113: 1377–1387, 2012. doi:10.1152/japplphysiol.01432.2011.
- Acute Respiratory Distress Syndrome N, Brower RG, Matthay MA, Morris A, Schoenfeld D, Thompson BT, Wheeler A. Ventilation with lower tidal volumes as compared with traditional tidal volumes for acute lung injury and the acute respiratory distress syndrome. *N Engl J Med* 342: 1301–1308, 2000. doi:10.1056/NEJM200005043421801.
- Hickling KG. The pressure-volume curve is greatly modified by recruitment. A mathematical model of ARDS lungs. *Am J Respir Crit Care Med* 158: 194–202, 1998. doi:10.1164/ajrccm.158.1.9708049.
- Maggiore SM, Jonson B, Richard JC, Jaber S, Lemaire F, Brochard L. Alveolar derecruitment at decremental positive end-expiratory pressure levels in acute lung injury: comparison with the lower inflection point, oxygenation, and compliance. *Am J Respir Crit Care Med* 164: 795–801, 2001. doi:10.1164/ajrccm.164.5.2006071.
- Allen G, Bates JH. Dynamic mechanical consequences of deep inflation in mice depend on type and degree of lung injury. *J Appl Physiol (1985)* 96: 293–300, 2004. doi:10.1152/japplphysiol.00270.2003.

14. **Massa CB, Allen GB, Bates JH.** Modeling the dynamics of recruitment and derecruitment in mice with acute lung injury. *J Appl Physiol* (1985) 105: 1813–1821, 2008. doi:10.1152/japplphysiol.90806.2008.

15. **Albert SP, DiRocco J, Allen GB, Bates JH, Lafollette R, Kubiak BD, Fischer J, Maroney S, Nieman GF.** The role of time and pressure on alveolar recruitment. *J Appl Physiol* (1985) 106: 757–765, 2009. doi:10.1152/japplphysiol.90735.2008.

16. **Gaver DP 3rd, Samsel RW, Solway J.** Effects of surface tension and viscosity on airway reopening. *J Appl Physiol* (1985) 69: 74–85, 1990. doi:10.1152/jappl.1990.69.1.74.

17. **Gaver DP, Halpern D, Jensen OE, Grotberg JB.** The steady motion of a semi-infinite bubble through a flexible-walled channel. *J Fluid Mech* 319: 25–65, 1996. doi:10.1017/S0022112096007240.

18. **Bates JHT, Gaver DP, Habashi NM, Nieman GF.** Atelectrauma versus volutrauma: a tale of two time-constants. *Crit Care Explor* 2: e0299, 2020. doi:10.1097/CCE.0000000000000299.

19. **Judge EP, Hughes JM, Egan JJ, Maguire M, Molloy EL, O'Dea S.** Anatomy and bronchoscopy of the porcine lung. A model for translational respiratory medicine. *Am J Respir Cell Mol Biol* 51: 334–343, 2014. doi:10.1165/rmbc.2013-0453TR.

20. **Slutsky AS, Ranieri VM.** Ventilator-induced lung injury. *N Engl J Med* 369: 2126–2136, 2013 [Erratum in *N Engl J Med* 370: 1668–1669, 2014]. doi:10.1056/NEJMra1208707.

21. **Jain SV, Kollisch-Singule M, Satalin J, Searles Q, Dombert L, Abdel-Razek O, Yeruvi N, Leonard A, Gruessner A, Andrews P, Fazal F, Meng Q, Wang G, Gatto LA, Habashi NM, Nieman GF.** The role of high airway pressure and dynamic strain on ventilator-induced lung injury in a heterogeneous acute lung injury model. *Intensive Care Med Exp* 5: 25, 2017. doi:10.1186/s40635-017-0138-1.

22. **Dreyfuss D, Soler P, Basset G, Saumon G.** High inflation pressure pulmonary edema. Respective effects of high airway pressure, high tidal volume, and positive end-expiratory pressure. *Am Rev Respir Dis* 137: 1159–1164, 1988. doi:10.1164/ajrccm.137.5.1159.

23. **Habashi NM.** Other approaches to open-lung ventilation: airway pressure release ventilation. *Crit Care Med* 33: S228–S240, 2005. doi:10.1097/01.ccm.0000155920.11893.37.

24. **Bates JHT.** *Lung Mechanics. An Inverse Modeling Approach.* Cambridge, UK: Cambridge University Press, 2009.

25. **Kubiak BD, Albert SP, Gatto LA, Snyder KP, Maier KG, Vieux CJ, Roy S, Nieman GF.** Peritoneal negative pressure therapy prevents multiple organ injury in a chronic porcine sepsis and ischemia/reperfusion model. *Shock* 34: 525–534, 2010. doi:10.1097/SHK.0b013e3181e14cd2.

26. **Gaver DP 3rd, Nieman GF, Gatto LA, Cereda M, Habashi NM, Bates JHT.** The POOR Get POORer: a hypothesis for the pathogenesis of ventilator-induced lung injury. *Am J Respir Crit Care Med* 202: 1081–1087, 2020. doi:10.1164/rccm.202002-0453CP.

27. **Hamlington KL, Bates JHT, Roy GS, Julianelle AJ, Charlebois C, Suki B, Smith BJ.** Alveolar leak develops by a rich-get-richer process in ventilator-induced lung injury. *PLoS One* 13: e0193934, 2018. doi:10.1371/journal.pone.0193934.

28. **Sugita S, Kubo T, Aoyama T, Moriya J, Okuni T, Wanibuchi M, Yamashita K, Onodera M, Tsujiwaki M, Segawa K, Sugawara T, Hasegawa T.** Imprint cytology of biphenotypic sinonasal sarcoma of the paranasal sinus: a case report. *Diagn Cytopathol* 47: 507–511, 2019. doi:10.1002/dc.24142.

29. **Otto CM, Markstaller K, Kajikawa O, Karmrodt J, Syring RS, Pfeiffer B, Good VP, Frevert CW, Baumgardner JE.** Spatial and temporal heterogeneity of ventilator-associated lung injury after surfactant depletion. *J Appl Physiol* (1985) 104: 1485–1494, 2008. doi:10.1152/japplphysiol.01089.2007.

30. **Kollisch-Singule M, Emr B, Smith B, Ruiz C, Roy S, Meng Q, Jain S, Satalin J, Snyder K, Ghosh A, Marx WH, Andrews P, Habashi N, Nieman GF, Gatto LA.** Airway pressure release ventilation reduces conducting airway micro-strain in lung injury. *J Am Coll Surg* 219: 968–976, 2014. doi:10.1016/j.jamcollsurg.2014.09.011.

31. **Protti A, Andreis DT, Monti M, Santini A, Sparacino CC, Langer T, Votta E, Gatti S, Lombardi L, Leopardi O, Masson S, Cressoni M, Gattinoni L.** Lung stress and strain during mechanical ventilation: any difference between statics and dynamics? *Crit Care Med* 41: 1046–1055, 2013. doi:10.1097/CCM.0b013e31827417a6.

32. **Tremblay L, Valenza F, Ribeiro SP, Li J, Slutsky AS.** Injurious ventilatory strategies increase cytokines and c-fos mRNA expression in an isolated rat lung model. *J Clin Invest* 99: 944–952, 1997. doi:10.1172/JCI119259.

33. **Baumgardner JE, Markstaller K, Cm O.** High-frequency ventilation is not the optimal physiological approach to ventilate ARDS patients. *J Appl Physiol* (1985) 104: 1239, 2008. doi:10.1152/japplphysiol.00153.2008.

34. **Mertens M, Tabuchi A, Meissner S, Krueger A, Schirrmann K, Kertzscher U, Pries AR, Slutsky AS, Koch E, Kuebler WM.** Alveolar dynamics in acute lung injury: heterogeneous distension rather than cyclic opening and collapse. *Crit Care Med* 37: 2604–2611, 2009. doi:10.1097/CCM.0b013e3181a5544d.

35. **Marini JJ, Gattinoni L.** Time course of evolving ventilator-induced lung injury: the “shrinking baby lung”. *Crit Care Med* 48: 1203–1209, 2020. doi:10.1097/CCM.0000000000004416.

36. **Amato MB, Meade MO, Slutsky AS, Brochard L, Costa EL, Schoenfeld DA, Stewart TE, Briel M, Talmor D, Mercat A, Richard JC, Carvalho CR, Brower RG.** Driving pressure and survival in the acute respiratory distress syndrome. *N Engl J Med* 372: 747–755, 2015. doi:10.1056/NEJMsa1410639.

37. **Guerin C, Papazian L, Reignier J, Ayzac L, Loundou A, Forel JM; investigators of the Acurasys and Proseva trials.** Effect of driving pressure on mortality in ARDS patients during lung protective mechanical ventilation in two randomized controlled trials. *Crit Care* 20: 384, 2016. doi:10.1186/s13054-016-1556-2.

38. **Deans KJ, Minneci PC, Cui X, Banks SM, Natanson C, Eichacker PQ.** Mechanical ventilation in ARDS: One size does not fit all. *Crit Care Med* 33: 1141–1143, 2005. doi:10.1097/01.ccm.0000162384.71993.a3.

39. **Terragni PP, Rosboch G, Tealdi A, Corno E, Menaldo E, Davini O, Gandini G, Herrmann P, Mascia L, Quintel M, Slutsky AS, Gattinoni L, Ranieri VM.** Tidal hyperinflation during low tidal volume ventilation in acute respiratory distress syndrome. *Am J Respir Crit Care Med* 175: 160–166, 2007. doi:10.1164/rccm.200607-915OC.

40. **Gattinoni L, Pelosi P, Suter PM, Pedoto A, Vercesi P, Lissoni A.** Acute respiratory distress syndrome caused by pulmonary and extrapulmonary disease. Different syndromes? *Am J Respir Crit Care Med* 158: 3–11, 1998. doi:10.1164/ajrccm.158.1.9708031.

41. **De Santis Santiago R, Teggia Droghi M, Fumagalli J, Marrazzo F, Florio G, Grassi LG, Gomes S, Morais CCA, Ramos OPS, Bottiroli M, Pincioli R, Imber DA, Bagchi A, Shelton K, Sonny A, Bittner EA, Amato MBP, Kacmarek RM, Berra L; Lung Rescue Team Investigators.** High pleural pressure prevents alveolar overdistension and hemodynamic collapse in ARDS with acute respiratory distress syndrome with class III obesity. *Am J Respir Crit Care Med* 203: 575–584, 2021. doi:10.1164/rccm.201909-1687OC.

42. **Kollisch-Singule M, Emr B, Jain SV, Andrews P, Satalin J, Liu J, Porcellio E, Kenyon V, Wang G, Marx W, Gatto LA, Nieman GF, Habashi NM.** The effects of airway pressure release ventilation on respiratory mechanics in extrapulmonary lung injury. *Intensive Care Med Exp* 3: 35, 2015. doi:10.1186/s40635-015-0071-0.

43. **Kollisch-Singule M, Emr B, Smith B, Roy S, Jain S, Satalin J, Snyder K, Andrews P, Habashi N, Bates J, Marx W, Nieman G, Gatto LA.** Mechanical breath profile of airway pressure release ventilation: the effect on alveolar recruitment and microstrain in acute lung injury. *JAMA Surg* 149: 1138–1145, 2014. doi:10.1001/jamasurg.2014.1829.

44. **Cressoni M, Chiumello D, Carlesso E, Chiurazzi C, Amini M, Brioni M, Cadringher P, Quintel M, Gattinoni L.** Compressive forces and computed tomography-derived positive end-expiratory pressure in acute respiratory distress syndrome. *Anesthesiology* 121: 572–581, 2014. doi:10.1097/ALN.0000000000000373.

45. **Cressoni M, Chiurazzi C, Gotti M, Amini M, Brioni M, Algieri I, Cammarotto A, Rovati C, Massari D, di Castiglione CB, Nikolla K, Montaruli C, Lazzarini M, Dondossola D, Colombo A, Gatti S, Valerio V, Gagliano N, Carlesso E, Gattinoni L.** Lung inhomogeneities and time course of ventilator-induced mechanical injuries. *Anesthesiology* 123: 618–627, 2015. doi:10.1097/ALN.0000000000000727.

46. **Mead J, Takishima T, Leith D.** Stress distribution in lungs: a model of pulmonary elasticity. *J Appl Physiol* 28: 596–608, 1970. doi:10.1152/jappl.1970.28.5.596.

47. **Cressoni M, Cadringher P, Chiurazzi C, Amini M, Gallazzi E, Marino A, Brioni M, Carlesso E, Chiumello D, Quintel M, Bugeo G, Gattinoni L.** Lung inhomogeneity in patients with acute respiratory distress syndrome. *Am J Respir Crit Care Med* 189: 149–158, 2014. doi:10.1164/rccm.201308-1567OC.



48. **Shono A, Kotani T.** Clinical implication of monitoring regional ventilation using electrical impedance tomography. *J Intensive Care* 7: 4, 2019. doi:10.1186/s40560-019-0358-4.
49. **Nieman GF, Gatto LA, Andrews P, Satalin J, Camporota L, Daxon B, Blair SJ, Al-Khalisy H, Madden M, Kollisch-Singule M, Alesh H, Habashi NM.** Prevention and treatment of acute lung injury with time-controlled adaptive ventilation: physiologically informed modification of airway pressure release ventilation. *Ann Intensive Care* 10: 3, 2020. doi:10.1186/s13613-019-0619-3.
50. **Nieman GF, Al-Khalisy H, Kollisch-Singule M, Satalin J, Blair S, Trikha G, Andrews P, Madden M, Gatto LA, Habashi NM.** A physiologically informed strategy to effectively open, stabilize, and protect the acutely injured lung. *Front Physiol* 11: 227, 2020. doi:10.3389/fphys.2020.00227.